Theoretical, spectral characterization and antineoplastic activity of new lanthanide complexes

ARTICLE *in* JOURNAL OF TRACE ELEMENTS IN MEDICINE AND BIOLOGY · FEBRUARY 2008

Impact Factor: 2.37 · DOI: 10.1016/j.jtemb.2007.10.005 · Source: PubMed

3 AUTHORS, INCLUDING:

N. Trendafilova
Bulgarian Academy of Sciences
84 PUBLICATIONS **776** CITATIONS

SEE PROFILE

Georgi Momekov
Medical University of Sofia
138 PUBLICATIONS **1,112** CITATIONS

SEE PROFILE

Available online at www.sciencedirect.com
ScienceDirect
Journal of Trace Elements in Medicine and Biology 22 (2008) 100–111
Journal of Trace Elements in Medicine and Biology
www.elsevier.de/jtemb

BIOINORGANIC CHEMISTRY

Theoretical, spectral characterization and antineoplastic activity of new lanthanide complexes

Irena Kostova[a,*], Natasha Trendafilova[b], Georgi Momekov[c]

[a]*Department of Chemistry, Faculty of Pharmacy, Medical University, 2 Dunav Street, Sofia 1000, Bulgaria*
[b]*Institute of General and Inorganic Chemistry, Bulgarian Academy of Sciences, 1113 Sofia, Bulgaria*
[c]*Laboratory of Experimental Chemotherapy, Department of Pharmacology and Toxicology, Faculty of Pharmacy, Medical University, 2 Dunav Street, Sofia 1000, Bulgaria*

Received 13 May 2007; accepted 14 October 2007

Abstract

The new cerium(III), lanthanum(III) and neodymium(III) complexes were synthesized in view of their application as cytotoxic agents. The complexes were characterized by different physicochemical methods: elemental analysis, mass spectrometry, ^{1}H NMR, ^{13}C NMR and IR spectroscopy. The spectra of the complexes were interpreted on the basis of comparison with the spectrum of the free ligand. The vibrational analysis showed that in the complexes the ligand coordinates to the metal ion through both deprotonated hydroxyl groups, however participation of the carbonyl groups in the coordination to the metal ion was also suggested. Geometry optimization of 3,3′-(*ortho*-pyridinomethylene)di-[4-hydroxycoumarin] H_2(*o*-pyhc), (H_2L) and its dianionic forms, *o*-pyhc^{2-}, (L^{2-}) were carried out at AM1 and PM3 levels as well as using density functional theory with Becke's three parameter hybrid method and correlation functional of Lee, Yang and Parr (B3LYP) with 6–31G(d) basis set. The optimized geometries of the neutral ligand isomers were stabilized by two asymmetrical intramolecular O–H...O hydrogen bonds (HBs). The conformational search showed four low-energy dianionic species (*o*-pyhc^{2-}) on the potential energy surface. Molecular electrostatic potential calculations showed that the most preferred sites for electrophilic attack in H_2(*o*-pyhc) and *o*-pyhc^{2-} are the carbonyl oxygen atoms. The evaluation of the cytotoxic activity of the novel lantanide complexes on HL-60 myeloid cells revealed, that they are potent cytotoxic agents. The cerium complex was found to exhibit superior activity in comparison to the lanthanum, and neodymium species, the latter being the least active. Taken together our data give us a reason to conclude that the newly synthesized lanthanide complexes should be a subset to further more detailed pharmacological and toxicological evaluation.

Keywords: 4-Hydroxycoumarins; Lanthanide(III) complexes; IR and NMR spectra; DFT; Cytotoxicity

Introduction

Chemistry of coordination compounds with biologically active ligands has received much attention during recent years. Coumarins are an important group of organic compounds showing wide variety of biological activity [1–5]. From the structural perspective, coumarins consist of a bicyclic system made up of a fused α-pyrone and benzene ring. Many substitution patterns are possible on the central bicyclic system giving rise to a variety of biological effects and various pharmacological and potential therapeutic properties have been

*Corresponding author. Tel.: +359 2 92 36 569; fax: +359 2 987 9874.
E-mail address: irenakostova@yahoo.com (I. Kostova).

0946-672X/$ - see front matter © 2007 Elsevier GmbH. All rights reserved.
doi:10.1016/j.jtemb.2007.10.005

attributed to coumarins [1–5]. Most of coumarin compounds have demonstrated numerous antitumor and antiproliferative effects [5]. Although coumarins have been used in anticancer therapy, little is known about the mechanism of action of these drugs. The study of coumarins is complex because of the heterogeneity of the different molecular structures and the scarcity of data on bioavailability. Coumarins and their derivatives have been also studied for their complexation with metal ions [6–9] and their complexes with rare-earth ions have aroused much interest.

Until 20 years ago, the results on antitumor therapy using lanthanides were not encouraging. Although the interest of researchers for lanthanide-based anticancer drugs was low for decades, a number of lanthanide complexes have been synthesized and their cytotoxicity was tested [10–13]. Lanthanide compounds are expected to be active in preventing tumor growth, since Ln competitively suppress iron uptake, inhibit ROS formation by binding to hydro-peroxides, masking the free radicals via magnetic interaction, intervening signal transduction, etc. Lanthanide ions are subjects of increasing interest in bioinorganic and coordination chemistry. At that time, studies of the coordination chemistry and the physical chemistry of the lanthanides were successful, but only a few, important, practical applications existed [10–14]. To this end, it is essential to understand the nature of these coordination compounds and their properties. Based on the small amount of available data, we know that the difference in the number of 4f electrons leads to quite different biological properties. It should be noted that in most experiments, the lanthanide used is selected only by tradition, for instance gadolinium and lanthanum [14].

Lanthanides manifest an antitumor activity [10,11] and furthermore, literature data show that the coumarins have also these properties [5,7,8]. These previous data from literature are in accordance with our investigations [14–20]. They give our reason to suppose that complexes of coumarins with lanthanides could present interesting organometalic compounds with antitumor activity. As a result from our earlier work the cytotoxic profile of some complexes of coumarin derivatives with lanthanides against different tumor cell lines was proved [14–20]. The corresponding lanthanide salts were found to be of very low or missing activity. So far we can conclude that the structure metal–ligand determines the antitumor spectrum of the newly complexes.

It was, therefore, considered worthwhile to study the complexation of cerium(III), lanthanum(III) and neodymium(III) with 3,3′-(*ortho*-pyridinomethylene)di-[4-hydroxycoumarin] and in the first place the objective of this study was to determine whether the new complexes were active as cytotoxic agents.

In the present study, we perform investigation of the coordination ability of 3,3′-(*ortho*-pyridinomethylene)-di-[4-hydroxycoumarin] in complexation reaction with cerium(III), lanthanum(III) and neodymium(III). The obtained lanthanide complexes were characterized by elemental analysis, physicochemical methods, mass-, NMR- and IR-spectroscopy. The most sensitive to coordination modes of the ligands have been assigned and discussed. The synthesis of lanthanide(III) complexes with 3,3′-(*ortho*-pyridinomethylene)di-[4-hydroxycoumarin] is taken into consideration with cytotoxic screening and further pharmacological study.

Materials and methods

Computational procedure

Conformational search was performed for the neutral and the dianionic forms of 3,3′-(*ortho*-pyridinomethylene)di-[4-hydroxycoumarin] (*o*-pyhc) using semi-empirical AM1 and PM3 methods. The geometry optimization of the neutral and dianionic ligand forms were further carried out using density functional theory with Becke's three parameter hybrid method and correlation functional of Lee, Yang and Parr (B3LYP) with 6–31G(d) basis set [21,22]. The geometry optimizations for the systems studied were carried out without constraints. The atomic charges were calculated using Natural Population Analysis (NPA) scheme [23]. All calculations of the systems studied were performed with Gaussian98 program package [24].

Further, we used the molecular electrostatic potential (MEP) as another fundamental determinant of atomic and molecular properties since it is rigorously related to the electronic density of the molecule. MEP has proven to be useful in rationalizing interactions between molecules and in molecular recognition processes since the electrostatic forces are primary responsible for long-range interactions [25,26]. MEP has largely been used as a molecular descriptor of the chemical reactivity of a number of biological systems which take part in both electrophilic and nucleophilic reactions as well as hydrogen bonding interactions [25,27,28]. The MEP, $V(\mathbf{r})$, at a given point $\mathbf{r}(x, y, z)$ in the vicinity of a molecule, is defined in terms of the interaction energy between the electrical charge generated from the molecule electrons and nuclei and a positive test charge (a proton) located at $\mathbf{r}$. For the systems studied the MEP values were calculated as described previously using the equation:

$$V(\mathbf{r}) = \sum_{A} \frac{Z_A}{|\mathbf{R}_A - \mathbf{r}|} - \int \frac{\rho(\mathbf{r}')}{|\mathbf{r}' - \mathbf{r}|} \, d\mathbf{r}' \quad (1)$$

where Z_A is the charge of nucleus A located at a distance $\mathbf{R}_A$, $\rho(\mathbf{r}')$ is the electronic density function

of the molecule, and $\mathbf{r}'$ is the dummy integration variable.

Chemistry

Synthesis of Ln(III) complexes with 3,3′-(*ortho*-pyridinomethylene)di-[4-hydroxycoumarin]

The compounds used for preparation of the solutions were Merck products, p.a. grade: $Ce(NO_3)_3 \cdot 6H_2O$, $La(NO_3)_3 \cdot 6H_2O$, $Nd(NO_3)_3 \cdot 6H_2O$. 3,3′-(*Ortho*-pyridinomethylene)di-[4-hydroxycoumarin] ($C_{24}H_{15}NO_6$, H_2L) was used for the preparation of metal complexes as ligand (Scheme 1).

The complexes of lanthanides(III) with 3,3′-(*ortho*-pyridinomethylene)di-[4-hydroxycoumarin] were synthesized by reaction of lanthanide(III) salts and the ligand, in amounts equal to metal:ligand molar ratio of 1:2. The ligand is insoluble in water. On raising the pH by the dropwise addition of a dilute solution of sodium hydroxide (0.1 mol/L) the ligand was dissolved. The complexes were prepared by adding aqueous solution of Ln(III) salts (1 mmol) to the solution of the ligand (2 mmol). The reaction mixtures were stirred with an electromagnetic stirrer at 25 °C. At the moment of mixing of the solutions, precipitates were obtained. The precipitates were filtered (pH of the filtrates was 5.0). The fawn precipitates were washed several times with water and dried in a desicator to constant weight. The complexes are insoluble in water, slightly soluble in methanol and ethanol and very soluble in DMSO.

Spectroscopic measurements

The elemental analyses for C, H, Ln and H_2O were performed according to standard microanalytical procedures. The IR spectra (Nujol and KBr) were recorded on IR-spectrometer FTIR-8101M Shimadzu (3800–400 cm^{-1}) and on IR-spectrometer Perkin-Elmer GX Auto image system (700–200 cm^{-1}). The ^1H NMR spectra were recorded at room temperature on Brucker WP 250 (250 MHz) spectrometer in DMSO-d_6. The ^{13}C NMR spectra were recorded at ambient temperature on Brucker 250 WM (62.9 MHz) spectrometer in DMSO-d_6. Chemical shifts are given in ppm, downfield from TMS. The mass-spectra were recorded on a Jeol JMS D 300 double focusing mass spectrometer coupled to a JMA 2000 data system. The compounds were introduced by direct inlet probe, heated from 50 to 400 °C at a rate of 100 °C/min. The ionization current was 300 mA, the accelerating voltage 3 kV and the chamber temperature 150 °C.

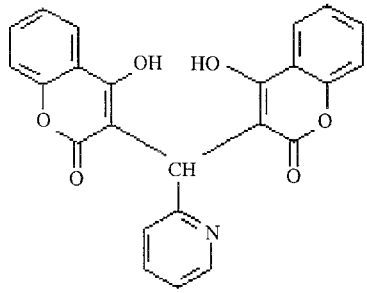

Scheme 1. Structure of the ligand 3,3′-(*ortho*-pyridinomethylene)di-[4-hydroxycoumarin].

Pharmacology

Human tumor cell lines and culture conditions

The antineoplastic activity of the tested compounds was assessed on the acute myeloid leukemia-derived HL-60 cell line; it was obtained from the Department of Human and Animal Cell Cultures at the German Collection of Microorganisms and Cell Cultures (DSMZ). The cells were grown as suspension-type cultures under standard conditions – RPMI 1640 medium (Sigma), supplemented with 10% heat inactivated fetal bovine serum (Sigma) and 2 mmol/L L-glutamine (Sigma), in a controlled environment – 'Heraeus' incubator with humidified atmosphere and 5% carbon dioxide, at 37 °C in cell culture flasks. In order to maintain the cells in log-phase cell suspension was discarded two to three times per week and the remaining culture was supplemented with fresh medium aliquots.

Cytotoxicity determination

All of the procedures concerning the stock solution preparation and cytotoxicity determination were carried out in a 'Heraeus' laminar flow cabinet. Stock solutions of the complexes under investigations were freshly prepared in DMSO and consequently diluted in RPMI 1640 medium in order to yield the desired final concentrations.

The cytotoxic activity of the investigated rare-earth complexes was assessed by the MTT [3-(4,5-dimethylthiazol-2-yl)-2,5diphenyltetrazolium bromide] dye reduction assay. Briefly, logarithmically growing cells were seeded into 96-well microplates (100 μL/well at a density of 1×10^5 cells/mL) and exposed to various concentrations of the investigated compounds for or 72 h. After the incubation with the test compounds MTT (3-(4,5-dimethylthiazol-2-yl)-2,5-diphenyltetrazolium bromide; Sigma) solution (10 mg/mL in PBS) was added (10 μL/well).

The absorption was measured using an ELISA reader (Uniscan Titertec) at wavelength of 580 nm. Plates were further incubated for 4 h at 37 °C and the formazan crystals formed were dissolved by adding 100 μL/well of 5% formic acid in 2-propanol. Absorption was measured by an ELISA reader (UniscanTitertek) at 540 nm,

reference filter 690 nm. For each concentration at least 8 wells were used. One hundred microliters RPMI 1640 medium with 10 μL MTT stock and 100 μL 5% formic acid in 2-propanol was used as blank solution.

Results and discussion

Chemistry

Molecular and geometrical structures of the neutral H_2(*o*-pyhc) and anionic *o*-pyhc^{2-} forms of the ligand

The molecular and geometrical structures of the neutral and dianionic ligand forms were studied in gas phase and in solution. Conformational analysis of the neutral and deprotonated forms of *ortho*-H_2(pyhc) was performed in gas phase using semi-empirical methods AM1 and PM3. For the neutral form both methods showed two low-energy isomers, which have a suitable orientation for intramolecular O–H...O hydrogen bonding, H_2(2-pyhc) and H_2(6-pyhc), Fig. 1a and b. For the dianionic forms, the calculations showed eight geometrical configurations. The AM1 and PM3 relative energy (stability) orders obtained showed some differences but four dianionic conformers showed always comparatively lower energy and they were selected for the calculations at the higher level of theory. Two neutral isomers, H_2(2-pyhc) and H_2(6-pyhc), as well as four dianionic conformers, Ion1, Ion2, Ion3 and Ion4 (Fig. 2), were further studied at B3LYP/6–31(d) level of the theory. This level of calculations was tested in our previous study of phenyl substituted di-coumarins and the results obtained showed a very good agreement with experimental structural parameters available [29]. To study the effect of the solvent on the relative energy order of the dianions studied, single point calculations were performed using the COSMO model (conductor-like screening solvation model) as implemented in Gaussian98 (keyword CPCM) [30]. The relative electronic energies (ΔE), ZPVE-corrected electronic energies (ΔE^{corr}) and the free energies in gas phase (ΔG) of the systems studied are given in Table 1. The relative electronic energies of dianions in solution (water) calculated at B3LYP/6–31(d) level of theory (ΔE^{CPCM}) is also presented in Table 1. A survey of the results in Table 1 showed that the free energy difference of the two neutral isomers only is 0.73 kJ/mol. The calculated relative electronic (and corrected electronic) energies of the dianionic forms revealed that their stability increased in the order:

for ΔE and ΔE^{corr} – Ion4 < Ion2 < Ion3 < Ion1

The calculated relative free energies and the relative energies in water solution exchange the positions of Ion3 and Ion2:

for ΔG and ΔE^{CPCM} – Ion4 < Ion3 < Ion2 < Ion1

From the orders given above one may conclude that Ion1 is the most stable conformer for the dianionic forms both in gas phase and in solution. The results in Table 1 show further that the relative electronic energies in solution (ΔE^{CPCM}) increased as compared to those in gas phase (ΔE): Ion2–1.74 → 8.92 kJ/mol; Ion3–1.19 → 9.77 kJ/mol; Ion4–2.55 → 15.47 kJ/mol (Table 1).

The optimized geometries and the calculated structural parameters of the neutral isomers showed two intramolecular hydrogen bondings formed between the hydroxyl hydrogens and the carbonyl oxygens (O10–H13...O27, O28–H31...O9), as it is shown in Fig. 1. As previously mentioned the hydrogen bondings formed stabilize the molecule and hold the coumarin fragments in fixed positions in relation to each other. In all deprotonated (dianionic) forms the hydrogen bondings are absent and simultaneous rotations of the coumarin moieties about C3–C18 and C21–C18 bonds as well as of the benzene about C_{18}–C_{37} bond occurred to avoid repulsion between the negative charges of the hydroxyl and carbonyl oxygen atoms. Due to the rotation, mentioned above, the geometries of the corresponding low-energy dianionic conformers are far from the geometry of the lowest energy neutral conformer (Fig. 2).

As it is seen from Fig. 2, the four dianionic forms of H_2(*o*-pyhc) differ as to the positions of the three planar parts of the molecule, the pyridine- and the two 4-hydroxycoumarin fragments. The rotation of the 4-hydroxycoumarin fragments with regard to the pyridine fragment (rotation about C3–C18 and C21–C18 bonds, Fig. 2) was described with the changes in two dihedral angles, C2–C3–C18–C37 and C20–C21–C18–C37. The rotation of the pyridine fragment with regard to the bis-coumarin fragment (rotation about the C37–C18 bond) was defined with the changes in the H36–C18–C37–N dihedral angle.

Selected structural parameters of H_2(*o*-pyhc) and *o*-pyhc^{2-} are presented in Table 2. The results in Table 2 show that differences were obtained in the dihedral angles, mentioned above. As compared to the neutral isomers (H_2(2-pyhc) and H_2(6-pyhc), Fig. 1a and b, respectively) the H36–C18–C37–N dihedral angle in all dianions significantly decreased and it was closer to its value in 6-pyhc (–85.39 < 19.62–36.81 < 99.90). The C2–C3–C18–C37 and C20–C21–C18–C37 dihedral angles change significantly going from the neutral to the dianions, the smallest changes were obtained for Ion2. The comparison of the bond distances of H_2(*o*-pyhc) with those in *o*-pyhc^{2-} forms showed that after deprotonation significant changes were obtained for R(C4–O10) and R(C22–O28) bond lengths. The C4–O10 bond length decreased from 1.327 to 1.324 Å

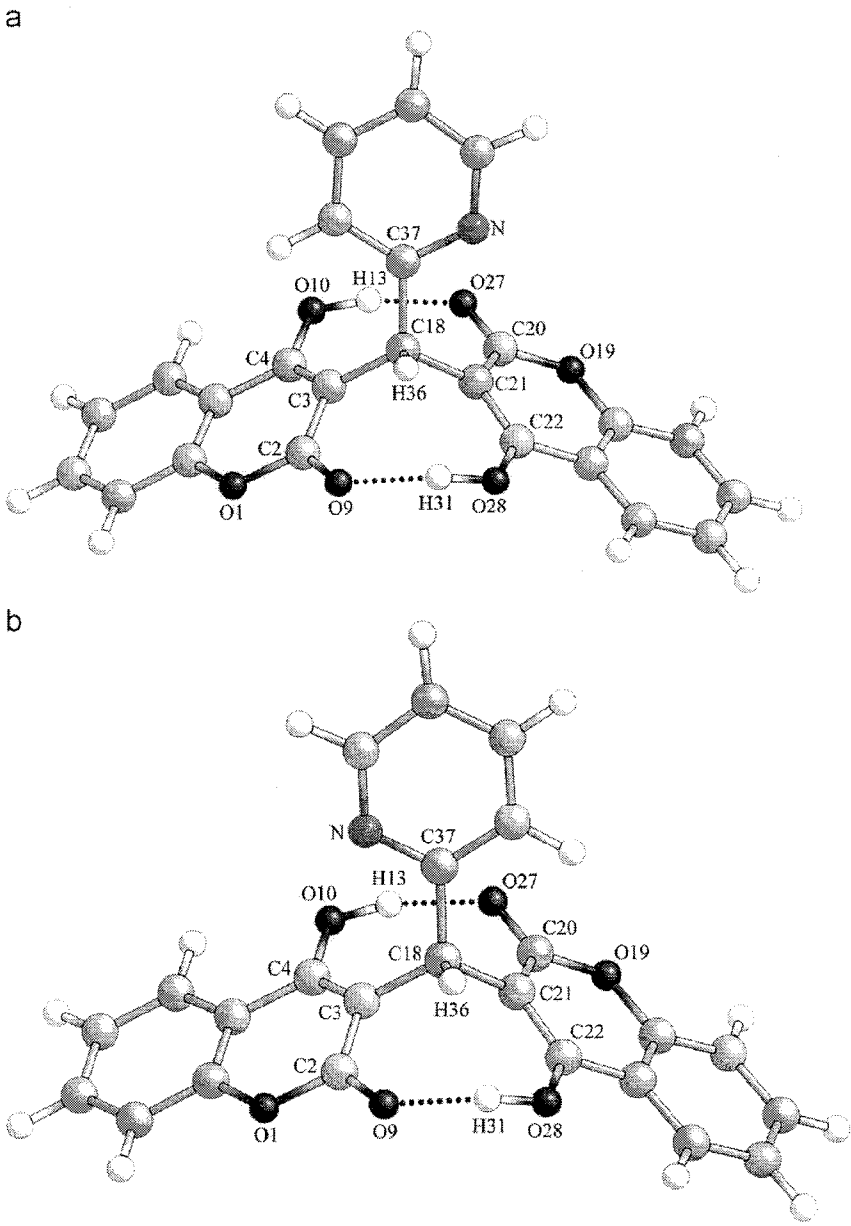

Fig. 1. Optimized molecular geometries of the two neutral ligand isomers: H_2(2-pyhc) and H_2(6-pyhc), obtained at B3LYP/6–31G(d) level of the theory.

in H_2(2-pyhc) and H_2(6-pyhc) to 1.254–1.256 Å in Ion1–Ion4. The same holds for C22–O28 bond distance, it decreased from 1.336 to 1.332 Å in H_2(2-pyhc) and H_2(6-pyhc) to 1.253–1.256 Å in the dianionic forms. As a result, the C–O and C=O bond length difference in the dianionic forms of the H_2(*o*-pyhc) significantly decreased in comparison with those in the neutral forms (Table 2).

The geometrical changes that occur in the neutral forms after deprotonation are due to the electron density distribution. To explain the C–O and C=O bond lengths equalization in the dianionic forms, we have studied the electronic structure changes. A suitable technique for this study was the Natural Bond Orbital (NBO) analysis. Since the four dianionic forms showed similar structures and not very large energy differences, we have selected for this study only the lowest-energy dianionic conformer, Ion1 (Fig. 2a). The results from the analysis made showed that in the deprotonated form (Ion1) a bonding interaction occurred between the p-orbitals of C4 and O10 as well as of C22 and O28 and as a result the π-character of the C4–O10 and

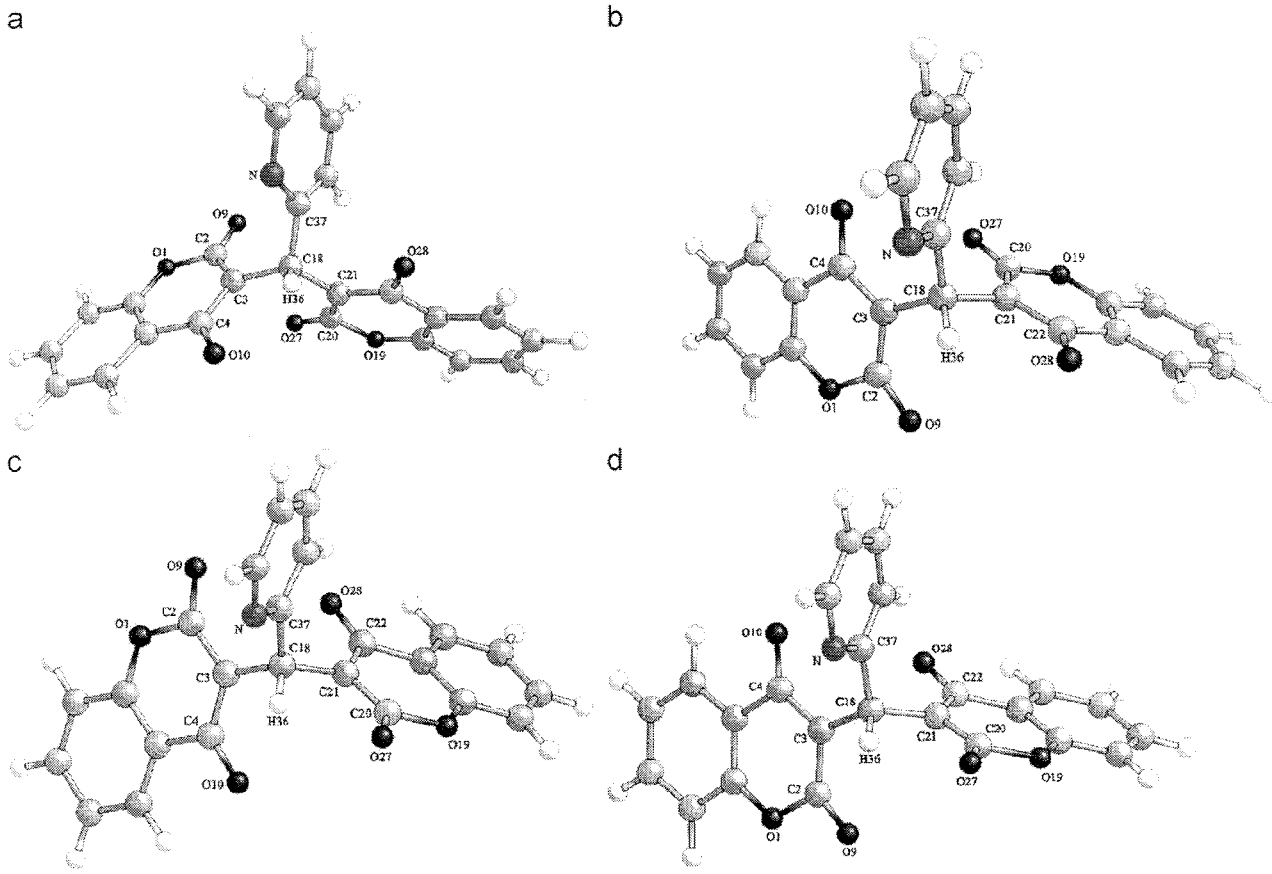

Fig. 2. Optimized molecular geometries of four low-energy dianionic ligand forms: Ion1 (a), Ion2 (b), Ion3 (c) and Ion4 (d), obtained at B3LYP/6–31G(d) level of theory.

Table 1. Relative energies (in kJ/mol) for neutral and dianionic forms of H_2(*o*-pyhc) in gas phase and water solution

Species	ΔE^{a}	ΔE^{corrb}	ΔG^{c}	ΔE^{CPCMd}
H_2(2-pyhc)	0.00	0.00	0.00	
H_2(6-pyhc)	1.13	1.17	0.73	
Ion1	0.00	0.00	0.00	0.00
Ion2	1.74	2.24	2.38	8.92
Ion3	1.19	2.10	3.90	9.77
Ion4	2.55	3.41	4.69	15.47

[a]Relative electronic energies in gas phase.
[b]Relative ZPVE corrected energies in gas phase.
[c]Relative free energies in gas phase.
[d]Relative electronic energies in water solution.

C22–O28 bonds increased. This finding explained the C–O and C=O bond lengths equalization in all the dianionic forms.

Atomic charges in the neutral H_2(*o*-pyhc) and deprotonated *o*-pyhc^{2-} ligand forms

Net atomic charges (q) of the neutral and deprotonated forms were calculated using the NPA (Table 3). In the neutral form, H_2(*o*-pyhc), the most negative charges were calculated for the hydroxylic oxygen atoms O10 and O28 (−0.691, −0.672 a.u.) followed by the carbonyl oxygen atoms O9 and O27 (−0.663, −0.639 a.u.). The nitrogen atomic charge was calculated significantly less negative as compared to the charges of the oxygen atoms (−0.467, −0.461 a.u., Table 3). The trend observed holds for the deprotonated dianionic forms (Ion1–4). The comparison between the neutral and dianionic forms showed that the largest charge changes occurred by the deprotonated oxygen atoms O10 and O28, they became more negative (in the range −0.709 to −0.689 a.u.). Despite the charge changes obtained in *o*-pyhc^{2-}, due to the significant charge delocalization the charge difference of O10, O28 on one side and O9, O27 on the other was not very large.

Molecular electrostatic potential (MEP)

There are several possible reactive sites in the neutral and the deprotonated forms of H_2(*o*-pyhc). To predict their relative reactivity in electrophilic or nucleophilic attack the MEP values were calculated and discussed. The negative regions of $V(r)$ are related to the

Table 2. Selected geometrical parameters (distance in Å, angles in deg) for H_2(*o*-pyhc) and *o*-pyhc^{2-} species calculated at B3LYP/6–31G(d) level of theory

Geometrical parameter[a]	H_2(2-pyhc)	H_2(6-pyhc)	Ion1	Ion2	Ion3	Ion4
C2–O9	1.232	1.236	1.223	1.223	1.222	1.223
C4–O10	1.327	1.324	1.256	1.254	1.254	1.254
C20–O27	1.231	1.230	1.217	1.223	1.222	1.223
C22–O28	1.336	1.332	1.256	1.253	1.256	1.256
C2–C3–C18–C37	134.27	132.48	−50.17	151.04	−27.84	156.11
C20–C21–C18–C37	49.97	49.08	118.75	86.60	−93.73	−95.32
H36–C18–C37–N	−85.39	99.90	36.81	25.16	21.46	19.62

[a]Atom numbering are given in Figs. 1 and 2.

Table 3. $V(r)$ values (a.u.) and atomic charges (q, a.u.) at selected atoms in the neutral and deprotonated forms of the ligand

Atom	H_2(2-pyhc)/H_2(6-pyhc)	*o*-pyhc^{2-}[a]
O9		
$V(r)$	−0.056/−0.059	−0.306
q	−0.663/−0.651	−0.656 to −0.650
O10		
$V(r)$	−0.033/−0.039	−0.297
q	−0.685/−0.672	−0.701 to −0.689
N		
$V(r)$	−0.053/−0.052	−0.29
q	−0.467/−0.461	−0.474 to −0.461
O27		
$V(r)$	−0.059/−0.057	−0.306
q	−0.645/−0.639	−0.654 to −0.628
O28		
$V(r)$	−0.036/−0.031	−0.294
q	−0.691/−0.690	−0.695 to −0.689

[a]$V(r)$ values at an atomic site in Ion1. Atomic charge interval for Ion1–4.

electrophilic reactivity and the positive regions of $V(r)$ to nucleophilic reactivity. The MEP values of the B3LYP/6–31G* optimized geometries of H_2(2-pyhc), H_2(6-pyhc) and Ion1 structures were calculated in agreement with Eq. (1). There is no rigorous basis for defining a molecular surface. Therefore, following the approach previously reported we have used those values of the MEP that correspond to the surface determined from points with electronic density $\rho(r) = 0.001$ e/Bohr^3 [31,32]. Selected MEP values are reported in Table 3. The advantage of such an approximation is that it reflects the specific features of the molecule, such as lone pair, strained bonds, etc. [32]. The electrostatic map was obtained at the equilibrium conformations. The most negative $V(\mathbf{r})$ values were associated with O9, O10, N, O27 and O28 atoms. For the neutral ligand, the $V(\mathbf{r})$ values increased in the order (in a.u):

$$O9, O27 < N < O10, O28$$

$$(-0.056 \text{ to } -0.059)(-0.052 \text{ to } -0.053)(-0.031 \text{ to } -0.039)\,\text{a.u.}$$

For Ion1 the MEP values on the corresponding atoms significantly decreased but their relative energy order does not change (in a.u.):

$$O9, O27 < N < O10, O28$$

$$(-0.306, -0.306)(-0.290)(-0.297, -0.294)$$

On the basis of the results thus obtained one may conclude that the most preferred sites for electrophilic attack in H_2(*o*-pyhc) and *o*-pyhc^{2-} are the carbonyl oxygen atoms, O9 and O27.

Coordination ability of 3,3′-(*ortho*-pyridinomethylene) di-[4-hydroxycoumarin] to Ln(III)

The elemental analysis data of the Ln(III) complexes obtained (Table 4) are in agreement with the formula, $Ln(L)(OH)\cdot nH_2O$, where $L = C_{24}H_{13}NO_6^{2-}$. The suggested formula was further confirmed by mass-spectral fragmentation analysis.

The characteristic peaks were observed in the mass spectra of the ligand and its metal complexes, which followed the similar fragmentation pattern as reported earlier [18–20]. The fragmentation of the ligand showed molecular ion peak (M + 1) at 413 and occurs via cleavage of organic moiety giving respective peaks to produce 4-hydroxycoumarin at m/z 162. As it is seen in Table 5, the mass spectra of the metal complexes show molecular ion peaks (M + 1) at m/z 586 and 585 for $Ce(L)(OH)\cdot H_2O$ and $La(L)(OH)\cdot H_2O$ complexes respectively and molecular peak at m/z 607 for $Nd(L)(OH)\cdot 2H_2O$, confirming their molecular weights. Elimination of metal, hydroxyl ion and water molecule was observed at m/z 410 for all of the complexes investigated, and further fragmentation followed a similar pathway as ligand. In the complex, elimination of one 4-hydroxycoumarin radical and a pyridyl radical

Table 4. Elemental analysis data for Ln(III) complexes with 3,3′-(*ortho*-pyridinomethylene)di-[4-hydroxycoumarin]

Complex	Found/calculated				
	% C	% H	% N	% H_2O	% Ln
$Ce(L)(OH)\cdot H_2O$	49.55	3.12	2.77	3.44	23.56
	49.15	2.75	2.39	3.07	23.89
$La(L)(OH)\cdot H_2O$	49.61	3.14	2.78	3.42	23.48
	49.25	2.76	2.39	3.08	23.73
$Nd(L)(OH)\cdot 2H_2O$	47.60	3.42	2.64	6.38	23.45
	47.36	2.98	2.30	5.92	23.69

$L = C_{24}H_{13}NO_6^{2-}$.

Table 5. Mass-spectral data of 3,3′-(*ortho*-pyridinomethylene)di-[4-hydroxycoumarin] and its Ln(III) complexes

Ligand	*m/z*	%	Complex	*m/z*	%
$H_2L = C_{24}H_{15}NO_6$	413	7	$Ce(L)(OH)\cdot H_2O$	586	1
	395	2		490	3
	252	7		460	5
	162	30		410	2
	120	28		307	40
	92	38		176	100
$H_2L = C_{24}H_{15}NO_6$	413	7	$La(L)(OH)\cdot H_2O$	585	1
	395	2		490	4
	252	7		460	6
	162	30		410	1
	120	28		307	70
	92	38		176	100
$H_2L = C_{24}H_{15}NO_6$	413	7	$Nd(L)(OH)\cdot 2H_2O$	607	2
	395	2		573	4
	252	7		552	1
	162	30		411	1
	120	28		307	45
	92	38		176	100

gives rise to the formation of 3-methyl-4-hydroxycoumarin at *m/z* 176, which was observed as a base peak in the spectra of all the complexes. Although of low intensity, the first peaks in the spectra of the Ln(III) complexes correspond with the mass weight of the complex formation. The results thus obtained suggest metal:ligand ratio of 1:1 and they are in agreement with the data of the elemental analysis.

Vibrational study of the ligand and its Ln(III) complexes

The binding mode of the ligand to Ln(III) ion was further elucidated by analysis of the IR spectra of 3,3′-(*ortho*-pyridinomethylene)di-[4-hydroxycoumarin] and the complex formation.

The bands appear in the IR spectrum of 3,3′-(*ortho*-pyridinomethylene)di-[4-hydroxycoumarin] (H_2L) at 3122, 3060, 1696, 1635, 1608, 1539, 1489, 1181, 1164, 1111, 1039 cm^{-1}. The bands at 1696 and 1635 cm^{-1} can be attributed to the stretching vibrations of the carbonyl groups of the lacton rings. Bands at 1608 and 1539 cm^{-1} can be related to the stretching vibrations of the conjugated olefinic system. The vibrations at 1489 cm^{-1} correspond to the aromatic systems. Bands at 1620, 1559, 1505, 1410 cm^{-1} can be attributed to the stretching vibrations of pyridine and they remain almost the same in the complex.

A broad band, characteristic for ν(O–H) of coordinated water was observed in the spectra of the complexes at about 3400 cm^{-1}. The most notable change in the ligand spectral features when coordinated to Ln(III) is the observed C=O red shift. The ν(C=O) bands in the ligand spectrum exhibited a red shift of 40 cm^{-1} in the spectra of the complexes. This finding may be taken as evidence for participation of the C=O group in coordination to the metal ion. Further, a comparison between the ligand and complex IR spectra revealed that the absorption bands associated with the stretching ν(O–H) of the phenolic groups (observed at 3122 and 3060 cm^{-1} in the free ligand) disappeared in the Ln(III) complex spectra, indicating a loss of phenolic protons on complexation and thus forming a metal–oxygen bonds. The δ(COH) i.p. modes, which appeared at 1350 and 1332 cm^{-1} in the spectrum of the ligand were not observed in the spectra of the complexes with Ln(III) and thus supported the suggestion that the ligand coordinates to the metal through its deprotonated form, L^{2-}. The Ln(III) complex spectra showed new bands, in comparison with that of the free ligand, at 550–400 cm^{-1}, and they were assigned to metal–oxygen stretching vibrations, in agreement with the literature data [33]. The results of the IR spectra are presented in Table 6 and Fig. 3.

^{1}H and ^{13}C NMR study of 3,3′-(*ortho*-pyridinomethylene)di-[4-hydroxycoumarin] and its Ln(III) complexes

The Ln(III) complexes and 3,3′-(*ortho*-pyridinomethylene)di-[4-hydroxycoumarin] were further studied by their ^{1}H and ^{13}C NMR spectra. The changes of chemical shifts of the ^{1}H NMR spectra were observed in the complexes (Table 7) and they were attributed to coordination of the ligand to Ln(III). The chemical shifts of the protons vary in the lanthanide complexes, because of the shift properties of these metals.

Due to electron transfer from the hydroxyl and carbonyl oxygen atoms to Ln(III), chemical shifts to different ppm were observed for the neighboring C-4, C-3 and C-2 carbon atoms of the complexes and they confirmed the expected coordination of the ligand through both deprotonated hydroxyl and carbonyl oxygen atoms (Table 8). The other carbon atoms were only slightly affected from the coordination of the

Table 6. Selected experimental IR frequencies of 3,3′-(*ortho*-pyridinomethylene)di-[4-hydroxycoumarin] and its Ln(III) complexes (cm^{-1})[a]

Compound	νOH/H_2O	ν(C=O)	ν(C=C)	ν(Py)	ν(Ar)	δ(COH)	ν(C–O)	
$H_2L = C_{24}H_{15}NO_6$				1620			1181m	
	3122m	1696s	1608s	1559	1489m	1350m	1164m	770
	3060m	1635s	1539s	1505		1332m	1111s	751
				1410			1039m	
$Ce(L)(OH)\cdot H_2O$				1622			1212w	
	3400br	1652sh	1520s	1557	1436m	–	1150w	760
		1600s		1506			1109m	
				1419			1078w	
$La(L)(OH)\cdot H_2O$				1622			1211w	
	3400br	1652sh	1520s	1558	1436m	–	1151w	759
		1599s		1506			1108m	
				1419			1076w	
$Nd(L)(OH)\cdot 2H_2O$				1622			1212w	
	3400br	1652sh	1522s	1558	1436m	–	1150w	759
		1598s		1506			1109m	
				1418			1078w	

[a]br: broad, s: strong, m: medium, sh: shoulder, w: weak.

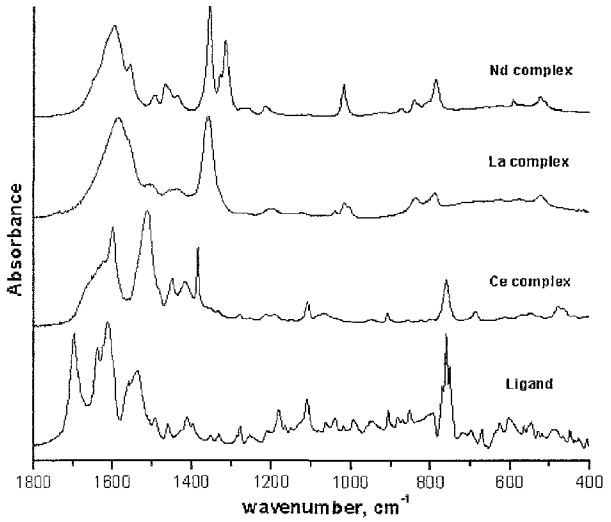

Fig. 3. FT-IR spectra of *o*-pyhc and its Ln(III) complexes.

metal. On the basis of the results thus obtained, it was suggested that the ligand acts as a tetradentate one in the Ln(III) complex formation.

Thus, on the basis of the experimental and theoretical results, we are able to suggest the most probable structure of the complexes (Fig. 4).

Pharmacology

In the present study, we investigated the cytotoxic effects of the three newly synthesized lanthanide complexes against the human leukemic cell lines HL-60 (human promuelocytic leukemia) using the standard MTT-dye reduction assay for cell viability.

The data for the cytotoxic efficacy of the tested compounds on HL-60 cells indicated that Ce(L)$(OH)\cdot H_2O$ proved to be the most active cytotoxic compound (Fig. 5). As evident from the results obtained

Table 7. ^{1}H NMR spectral shifts of 3,3′-(*ortho*-pyridinomethylene)di-[4-hydroxycoumarin] and its Ln(III) complexes (250 MHz, DMSO-d_6), δ (ppm)

Compound	δ (ppm)		
	H_5–H_8^a	H_9^a	$H_{3'}$–$H_{6'}^a$
$H_2L = C_{24}H_{15}NO_6$	7.24–7.58	6.54	7.80–8.64
$Ce(L)(OH)\cdot H_2O$	7.17–7.78	6.30	8.29–8.64
$La(L)(OH)\cdot H_2O$	7.15–7.81	6.30	8.03–8.33
$Nd(L)(OH)\cdot 2H_2O$	7.20–7.75	6.30	8.35–8.81

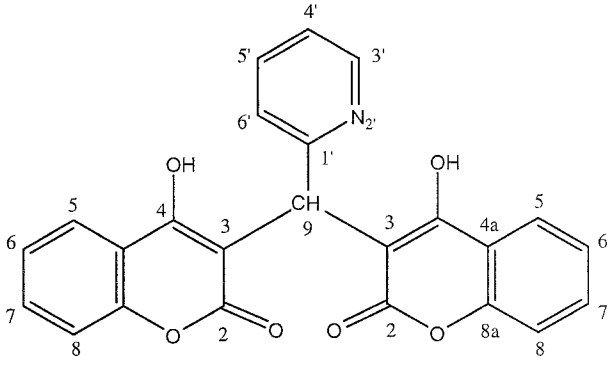

Table 8. ^{13}C NMR spectral shifts, δ (ppm) of 3,3′-(*ortho*-pyridinomethylene)di-[4-hydroxycoumarin] and its Ln(III) complexes (62.9 MHz, DMSO-d_6)

Atom	δ (ppm)			
	H_2L	$Ce(L)(OH)\cdot H_2O$	$La(L)(OH)\cdot H_2O$	$Nd(L)(OH)\cdot 2H_2O$
C-2	168.6	164.9	164.2	164.8
C-4	164.0	162.0	161.4	161.9
C-8a	157.6	156.6	152.2	157.28
C-1′	152.9	152.7	152.1	152.58
C-7	146.5	148.5	148.3	148.3
C-3′	141.9	136.0	136.4	135.8
C-5′	141.9	131.1	135.4	135.8
C-4′	131.9	126.3	130.5	130.3
C-6′	125.9	123.1	123.7	124.2
C-2′	–	–	–	–
C-5	124.4	121.1	122.2	122.4
C-6	123.4	120.2	120.5	120.4
C-4a	119.3	116.9	119.9	117.6
C-8	115.9	115.6	114.5	115.5
C-3	100.5	103.6	103.0	103.5
C-9	36.7	38.6	38.0	38.5

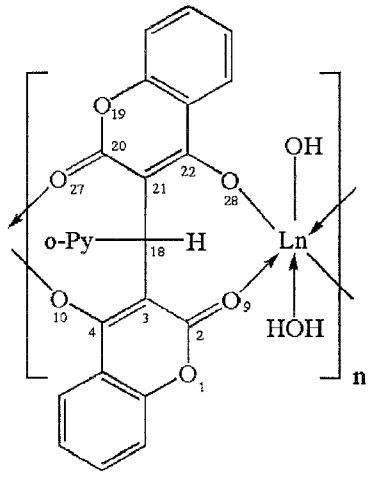

Fig. 4. The most probable structure of the Ln(III) complexes.

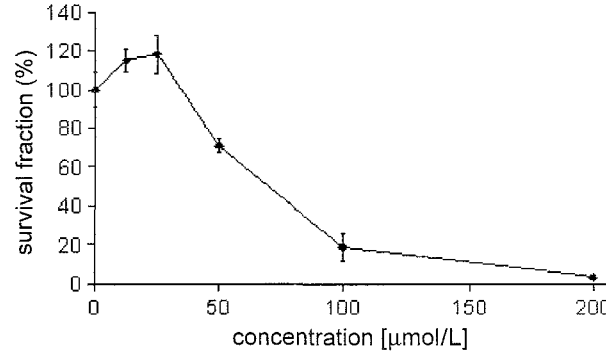

Fig. 5. Cytotoxic effects of $Ce(L)(OH)\cdot H_2O$ on HL-60 cells, as assessed by the MTT-dye reduction assay following 72 h treatment. Each data point represents the arithmetic mean ± S.D. of at least six independent experiments.

$Ce(L)(OH)\cdot H_2O$ exerted the most pronounced cytotoxic effects against the myeloid HL-60 cells with IC_{50} value of ca. 70 μmol/L. Whereas at concentrations up to 25 μmol/L certain increase of the cell survival was encountered, at 50 μmol/L $Ce(L)(OH)\cdot H_2O$ produced a 30% reduction of the percentage of viable HL-60 cells. At 100 μmol/L concentration $Ce(L)(OH)\cdot H_2O$ decreased the cell survival fraction by ca. 81%. When applied at the highest concentration investigated (200 μmol/L) it caused an almost absolute eradication of the malignant cells (survival fraction = ca. 3.12%). The other complexes under investigation were far less active against HL-60 with practical lack of cytotoxicity within the concentration range of 12.5–50 μmol/L (Figs. 6 and 7). The lanthanum complex under investigation also exerted concentration-dependent cytotoxic activity, though proved to be less potent than the corresponding cerium analogue on the basis of the IC_{50} value obtained. At the highest concentration of 200 μM applied $La(L)(OH)\cdot H_2O$ profound maximal efficacy with less than 10% viable leukemic cells. The third novel rare-earth coordination compound evaluated $Nd(L)(OH)\cdot 2H_2O$ showed the least cytotoxic activity.

The corresponding lanthanide salts and the ligand are found to be of very low or missing activity on these cells [19,34] which is in contrast to the lanthanide(III) complexes. So far we can conclude that the structure metal–ligand determines the antitumor spectrum of the newly synthesized lanthanide(III) complexes.

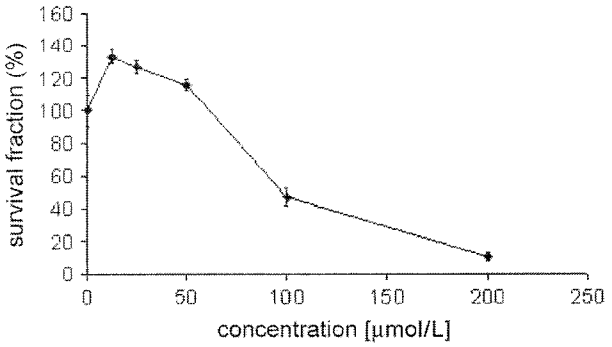

Fig. 6. Cytotoxic effects of La(L)(OH) · H_2O as assessed by the MTT-dye reduction assay following 72 h treatment of HL-60. Each data point represents the arithmetic mean ± S.D. of at least six independent experiments.

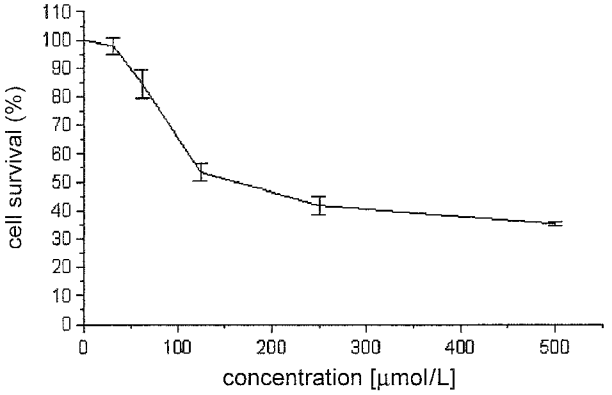

Fig. 7. Cytotoxic activity of Nd(L)(OH) · $2H_2O$ on HL-60 cells after 72 h incubation as assessed by MTT assay. Each data point represents the arithmetic mean of at least six independent experiments.

The observed in vitro effects are not so clearly expressed as in the case of *cis*-DDP(II) and other Ln(III) complexes presented by us earlier [14–20]. Nevertheless, their study is interesting in connection with other cell lines and tumors in order to find out differences in their spectrum of activity in comparison to other active lanthanide(III) complexes.

Conclusions

The coordination ability of 3,3′-(*ortho*-pyridinomethylene)di-[4-hydroxycoumarin] was proved in complexation reaction with lanthanide(iii) ions. ^{1}H, ^{13}C NMR and IR spectral analysis of the ligand and its Ln(III) complexes confirmed the suggested coordination of 3,3′-(*ortho*-pyridinomethylene)di-[4-hydroxycoumarin] through both the hydroxyl and carbonyl oxygen atoms.

Finally, the overall results from the preliminary screening program revealed, that all of the novel lantanide complexes with 3,3′-(*ortho*-pyridinomethylene)di-[4-hydroxycoumarin] are potent cytotoxic agents, although significant differences in their relative potencies were found in respect of the IC_{50} values obtained. The cerium complex was of superior activity in comparison to the lanthanum and neodymium species, the latter being the least active. Taken together our data give us reason to conclude that the newly synthesized lanthanide complexes should be subset to further more detailed pharmacological and toxicological evaluation.

Acknowledgment

The authors thank Dr. I. Manolov for the ligand supplied.

References

[1] Cálgaro-Helena AF, Devienne KF, Rodrigues T, Dorta DJ, Raddi MSG, Vilegas W, et al. Effects of isocoumarins isolated from Paepalanthus bromelioides on mitochondria: uncoupling, and induction/inhibition of mitochondrial permeability transition. Chem Biol Int 2006;161:155–64.

[2] Lee JH, Bang HB, Han SY, Jun J-G. An efficient synthesis of (+)-decursinol from umbelliferone. Tetrahedron Lett 2007;48:2889–92.

[3] Devienne KF, Cálgaro-Helena AF, Dorta DJ, Prado IMR, Raddi MSG, Vilegas W, et al. Antioxidant activity of isocoumarins isolated from Paepalanthus bromelioides on mitochondria. Phytochemistry 2007;68:1075–80.

[4] Yu J, Wang L, Walzem RL, Miller EG, Pike LM, Patil BS. Antioxidant activity of citrus limonoids, flavonoids, and coumarins. J Agric Food Chem 2005;53:2009–14.

[5] Thati B, Noble A, Creaven BS, Walsh M, McCann M, Kavanagh K, et al. A study of the role of apoptotic cell death and cell cycle events mediating the mechanism of action of 6-hydroxycoumarin-3-carboxylatosilver in human malignant hepatic cells. Cancer Lett 2007;250:128–39.

[6] Creaven BS, Egan DA, Kavanagh K, McCann M, Noble A, Thati B, et al. Synthesis, characterization and antimicrobial activity of a series of substituted coumarin-3-carboxylatosilver(I) complexes. Inorg Chim Acta 2006;359:3976–84.

[7] Budzisz E, Małecka M, Lorenz I-P, Mayer P, Kwiecień RA, Paneth P, et al. Synthesis, cytotoxic effect, and structure–activity relationship of Pd(II) complexes with coumarin derivatives. Inorg Chem 2006;45:9688–95.

[8] Thati B, Noble A, Creaven BS, Walsh M, McCann M, Kavanagh K, et al. In vitro anti-tumour and cyto-selective effects of coumarin-3-carboxylic acid and three of its hydroxylated derivatives, along with their silver-based complexes, using human epithelial carcinoma cell lines. Cancer Lett 2007;248:321–31.

[9] Nath M, Jairath R, Eng G, Song X, Kumar A. Triorganotin(IV) derivatives of umbelliferone (7-hydroxycoumarin) and their adducts with 1,10-phenanthroline: synthesis, structural and biological studies. J Organomet Chem 2005;690:134–44.
[10] Jakupec MA, Unfried P, Keppler BK. Pharmacological properties of cerium compounds. Rev Physiol Biochem Pharmacol 2005;153:101–11.
[11] Yin F, Zou J, Xu L, Wang X, Li R. Synthesis, characterization and antitumor activity of lanthanum(III) complex with demethylcantharidate. J Rare Earths 2005; 23:596–9.
[12] Bastos CC, Freire RO, Rocha GB, Simas AM. Sparkle model for AM1 calculation of neodymium(III) coordination compounds. J Photochem Photobiol A: Chem 2006;177:225–37.
[13] Brunet E, Juanes O, Sedano R, Rodriguez-Ubis JC. Lanthanide complexes of new polyaminocarboxylates with the bis-pyrazolylpyrimidine chromophore. Tetrahedron Lett 2007;48:1091–4.
[14] Kostova I. Lanthanides as anticancer agents. Curr Med Chem: Anti-Cancer Agents 2005;5:591–602.
[15] Kostova I, Manolov I, Nicolova I, Danchev N. New metal complexes of 4-methyl-7-hydroxycoumarin sodium salt and their pharmacological activity. Il Farmaco 2001;56:707–13.
[16] Kostova I, Manolov I, Nicolova I, Konstantinov S, Karaivanova M. New lanthanide complexes of 4-methyl-7-hydroxycoumarin and their pharmacological activity. Eur J Med Chem 2001;36:339–47.
[17] Kostova I, Manolov I, Konstantinov S, Karaivanova M. Synthesis, physicochemical characterisation and cytotoxic screening of new complexes of Ce, La and Nd with Warfarin and Coumachlor sodium salts. Eur J Med Chem 1999;34:63–8.
[18] Kostova I, Trendafilova N, Momekov G. Theoretical and spectroscopic evidence for coordination ability of 3,3′-benzylidenedi-4-hydroxycoumarin. New neodymium(III) complex and its cytotoxic effect. J Inorg Biochem 2005;99:477–87.
[19] Kostova I, Kostova R, Momekov G, Trendafilova N, Karaivanova M. Antineoplastic activity of new lanthanide (cerium, lanthanum and neodymium) complex compounds. J Trace Elem Med Biol 2005;18:219–26.
[20] Kostova I, Trendafilova N, Mihaylov T. Theoretical and spectroscopic studies of pyridyl substituted bis-coumarins and their new neodymium(III) complexes. Chem Phys 2005;314:73–84.
[21] Becke AD. Density-functional thermochemistry. III. The role of the exact exchange. J Chem Phys 1993;98:5648–52.
[22] Lee C, Yang W, Parr RG. Development of the Colle-Salvetti correlationenergy formula into a functional of the electron density. Phys Rev 1998;B37:785–9.
[23] Rablen PR, Lockman JW, Jorgensen WL. Ab initio study of hydrogenbonded complexes of small organic molecules with water. J Phys Chem A 1998;102:3782–97.
[24] Frisch MJ, Trucks GW, Schlegel HB, Scuseria GE, Robb MA, Cheeseman JR, et al. Gaussian98. Pittsburgh, PA: Gaussian Inc.; 1998. p. A.7.
[25] Munoz-Caro C, Nino A, Senent ML, Leal JM, Ibeas S. Modelling of protonation processes in the acetohydroxamic acid. J Org Chem 2000;65:405–10.
[26] Miertus S, Scrocco E, Tomasi J. Perspective on "Electrostatic interactions of a solute with a continuum. A direct utilization of ab initio molecular potentials for the prevision of solvent effects". Chem Phys 1981;55:117–29.
[27] Okulik N, Jubert AH. Theoretical analysis of the reactive sites of non-steroidal anti-inflammatory drugs. Internet Electr J Mol Des 2003;2:1–13.
[28] Soliva R, Luque FJ, Orozeo M. Reliability of MEP and MEP-derived properties computed from DFT methods for molecules containing P, S and Cl. Theor Chem Acc 1997;98:42–9.
[29] Trendafilova N, Bauer G, Mihaylov T. DFT and AIM studies of intramolecular hydrogen bonds in dicoumarols. Chem Phys 2004;302:95–104.
[30] Barone V, Cossi M. Quantum calculation of molecular energies and energy gradients in solution by a conductor solvent model. J Phys Chem 1998;102:1995–2001.
[31] Bader RFW, Carroll MT, Cheeseman JR, Chang C. Properties of atoms in molecules-atomic volumes. J Am Chem Soc 1987;109:7968–71.
[32] Politzer P, Murray J. The fundamental nature and role of the electrostatic potential in atoms and molecules. Theor Chem Acta 2002;108:134–42.
[33] Lewis FD, Barancyk SV. Lewis acid catalysis of photochemical reactions. 8. Photodimerization and crosscycloaddition of coumarin. J Am Chem Soc 1989;111: 8653–61.
[34] Kostova I, Momekov G, Zaharieva M, Karaivanova M. Cytotoxic activity of new lanthanum(III) complexes of bis-coumarins. Eur J Med Chem 2005;40:542–51.